

# A Decoupled Channel Estimation Method for Beyond Diagonal RIS

Bruno Sokal, Fazal-E-Asim, André L. F. de Almeida, Hongyu Li, and Bruno Clerckx

**Abstract**—Beyond diagonal reconfigurable intelligent surface (BD-RIS) is a new architecture for RIS where elements are interconnected to provide more wave manipulation flexibility than traditional single-connected RIS, enhancing data rate and coverage. However, channel estimation for BD-RIS is challenging due to the more complex multiple-connection structure involving their scattering elements. To address this issue, this paper proposes a decoupled channel estimation method for BD-RIS that yields separate estimates of the involved channels to enhance the accuracy of the overall combined channel by capitalizing on its Kronecker structure. Starting from a least squares estimate of the combined channel and by properly reshaping the resulting filtered signal, the proposed algorithm resorts to a Khatri-Rao Factorization (KRF) method that teases out the individual channels based on simple rank-one matrix approximation steps. Numerical results show that the proposed decoupled channel estimation yields more accurate channel estimates than the classical least squares scheme.

**Index Terms**—Beyond diagonal RIS, channel estimation, Khatri-Rao factorization.

## I. INTRODUCTION

A recent advancement over the conventional reconfigurable intelligent surface (RIS) technology, which uses diagonal phase shift matrices [1], [2], is the beyond diagonal reconfigurable intelligent surface (BD-RIS) which proved to achieve enhanced channel gain and enlarged coverage [3]–[5]. Interconnecting elements via additional tunable components enables BD-RIS to mathematically generate scattering matrices with nonzero off-diagonal entries, increasing the flexibility to manipulate waves. It is worth noting that the enhanced performance of BD-RIS architectures and modes depends highly on the accuracy of the channel state information (CSI). However, it is difficult to effectively and efficiently acquire the CSI for BD-RIS-aided wireless systems due to the lack of signal processing capabilities, from which, as the conventional RIS, the combined TX-RIS-RX channel is often estimated [6]–[8]. Also, the BD-RIS has additional physical constraints due to the physical connections, imposing a challenge on the design of the training BD-RIS matrix.

For conventional RIS-assisted systems, a traditional least squares (LS) based method has been proposed for combined TX-RIS-RX channel estimation. Although LS methods demonstrate good performance in terms of normalized mean square error (NMSE), LS methods often suffer from long pilot overhead and do not exploit the intrinsic structure of the combined TX-RIS-RX channel. In [8], [9], the authors proposed a decoupled channel estimation method that exploits the structure of the combined TX-RIS-RX channel. Their proposed method relies on tensor-based signal processing due

to the ability of tensor tools to fully exploit different signal diversity *dimensions* (e.g., space, time, frequency, polarization, etc.) [10]–[13]. In this sense, several works have adopted tensor-based methods for channel estimation [14]–[16]. In [14], the authors proposed a tensor-based approach for RIS-assisted multi-user MISO systems. The work [15] proposed a tensor-based framework for parametric estimation of low-rank channels. In [16], the authors proposed a tensor-based method for channel estimation and data in time-varying channels. Also, tensor-based methods can be employed in different applications in RIS-assisted systems, e.g., in [17], the authors introduced a tensor-based method that decouples the optimum phase shift vector of the RIS into multiple smaller factors, reducing the total required control signaling overhead between the network control and the RIS.

For BD-RIS, few works in the literature addressed the channel estimation problem [18], [19]. The work [18] has proposed a baseline LS based receiver to estimate the combined channel based on an orthogonal BD-RIS training matrix design that fulfills the BD-RIS physical constraints. In [19], the authors proposed a tensor-based approach for channel estimation and design of the BD-RIS training matrix, where an iterative and a closed-form-based receiver is proposed.

In this paper, we formulate a decoupled channel estimation method for MIMO BD-RIS systems. We consider the same system aspect and BD-RIS training design as the one proposed in the baseline LS solution [18]. Starting from the LS estimate of the combined channel and by exploiting its Kronecker decomposition structure, we resort to a Khatri-Rao Factorization (KRF) method that reveals the individual channels based on simple rank-one matrix approximation steps. The proposed method is conceptually simple and can be executed at low complexity since it relies on *permute* and *reshaping* operations on the filtered signal followed by multiple independent rank-one approximations. Interestingly, it is built up on the same principle as the Khatri-Rao Factorization (KRF) algorithm proposed earlier in [8] for traditional single-connected RIS. Otherwise stated, the proposed decoupled BD-RIS channel estimation method can be viewed as a general approach that encompasses the single-connected RIS to the group and fully-connected RIS (BD-RIS). Numerical results corroborate the effectiveness of the proposed method to provide accurate and individual channel estimates for BD-RIS.

## II. NOTATION AND PROPERTIES

Scalars are represented as non-bold lower-case letters  $a$ , column vectors as lower-case boldface letters  $\mathbf{a}$ , matrices as

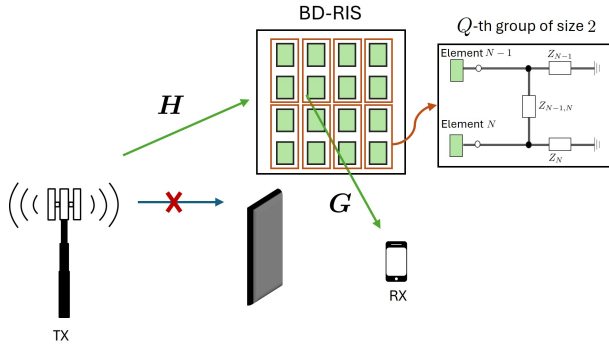


Fig. 1: BD-RIS assisted communication scenario.

upper-case boldface letters  $\mathbf{A}$ . The superscripts  $\{\cdot\}^T$ ,  $\{\cdot\}^*$ ,  $\{\cdot\}^H$  stand for transpose, conjugate, conjugate transpose. An identity matrix of dimension  $K$  is denoted as  $\mathbf{I}_K$ . The operator  $\|\cdot\|_F$  denotes the Frobenius norm of a matrix or tensor, and  $\mathbb{E}\{\cdot\}$  is the expectation operator. The operator  $\text{diag}(\mathbf{a})$  converts  $\mathbf{a}$  into a diagonal matrix, while  $\text{diag}(\mathbf{A})$  returns a vector whose elements are the main the diagonal of  $\mathbf{A}$ . Given a matrix  $\mathbf{A} \in \mathbb{C}^{I \times R}$ , the operator  $\text{D}_i(\mathbf{A})$  defines a diagonal matrix of size  $R \times R$  constructed from the  $i$ -th row of  $\mathbf{A}$ , for  $i \in \{1, \dots, I\}$ . From a set of  $Q$  matrices  $\mathbf{X}^{(q)} \in \mathbb{C}^{M \times N}$ ,  $q = \{1, \dots, Q\}$ , we can construct a block diagonal matrix as  $\mathbf{X} = \text{bdiag}(\mathbf{X}^{(1)}, \dots, \mathbf{X}^{(Q)}) \in \mathbb{C}^{MQ \times NQ}$ . Moreover,  $\text{vec}(\mathbf{A})$  converts  $\mathbf{A} \in \mathbb{C}^{I \times R}$  to a column vector  $\mathbf{a} \in \mathbb{C}^{IR \times 1}$  by stacking its columns on top of each other, while the operator  $\text{unvec}(\mathbf{a})_{I \times R}$  returns to the matrix  $\mathbf{A} \in \mathbb{C}^{I \times R}$ . The symbols  $\circ$ ,  $\otimes$ , and  $\diamond$  denote the outer product, the Kronecker product, and the Khatri-Rao product (also known as the column-wise Kronecker product), respectively. For example, the Khatri-Rao product of matrices  $\mathbf{X} \in \mathbb{C}^{I \times R}$  and  $\mathbf{Y} \in \mathbb{C}^{J \times R}$ , is defined as

$$\mathbf{Z} = \mathbf{X} \diamond \mathbf{Y} = [\mathbf{x}_1 \otimes \mathbf{y}_1, \dots, \mathbf{x}_R \otimes \mathbf{y}_R] \in \mathbb{C}^{JI \times R}, \quad (1)$$

where  $\mathbf{x}_r$  and  $\mathbf{y}_r$  are the  $r$ -th column of  $\mathbf{X}$  and  $\mathbf{Y}$ , respectively, for  $r = \{1, \dots, R\}$ . Useful properties that will be exploited in this paper are

$$\text{vec}(\mathbf{ABC}) = (\mathbf{C}^T \otimes \mathbf{A}) \text{vec}(\mathbf{B}), \quad (2)$$

$$\text{vec}(\mathbf{A} \text{diag}(\mathbf{b}) \mathbf{C}) = (\mathbf{C}^T \diamond \mathbf{A}) \mathbf{b}, \quad (3)$$

$$\text{vec}(\mathbf{A} \otimes \mathbf{B}) = \mathbf{P}(\text{vec}(\mathbf{A}) \otimes \text{vec}(\mathbf{B})) \quad (4)$$

$$\text{vec}(\mathbf{ab}^T) = \mathbf{b} \otimes \mathbf{a} \quad (5)$$

where the involved vectors and matrices have compatible dimensions in each case, and  $\mathbf{P}$  is a permutation matrix.

### III. SYSTEM MODEL

We consider a multiple-input multiple-output (MIMO) system assisted by a BD-RIS, where the transmitter and the receiver are equipped with  $M_T$  and  $M_R$  antennas, respectively, and a BD-RIS with  $N$  elements, illustrated in Figure 1. We assume the direct link between the transmitter and the receiver is blocked. Assuming a length- $T$  pilot sequence, the received signal at the  $t$  time slot is given by  $\mathbf{y}_t = \mathbf{G} \mathbf{S}_t \mathbf{H}^T \mathbf{x}_t + \mathbf{b}_t \in$

$\mathbb{C}^{M_R \times 1}$ , where  $\mathbf{G} \in \mathbb{C}^{M_R \times N}$  and  $\mathbf{H} \in \mathbb{C}^{M_T \times N}$  are the IRS-RX and the TX-IRS channels respectively, and  $\mathbf{b}_t$  is the additive white Gaussian noise (AWGN) term, with zero mean and unit variance.  $\mathbf{S}_t \in \mathbb{C}^{N \times N}$  is the BD-RIS scattering matrix, with  $\mathbf{S}_t^H \mathbf{S}_t = \mathbf{I}_N$ . Assuming a group connected BD-RIS architecture [5], the  $N$  elements are divided into  $Q$  groups with size  $\bar{N}$ , i.e.,  $N = \bar{N}Q$ . In this case, the scattering matrix can be written as  $\mathbf{S}_t = \text{bdiag}(\mathbf{S}_t^{(1)}, \dots, \mathbf{S}_t^{(Q)}) \in \mathbb{C}^{N \times N}$ . Due to the physical constraints of the BD-RIS group connections, the  $q$ -th scattering matrix  $\mathbf{S}_t^{(q)}$  must satisfy  $\mathbf{S}_t^{(q)H} \mathbf{S}_t^{(q)} = \mathbf{I}_{\bar{N}}$ . Thus, the received signal can be written as

$$\mathbf{y}_t = \sum_{q=1}^Q \mathbf{G}^{(q)} \mathbf{S}_t^{(q)} \mathbf{H}^{(q)T} \mathbf{x}_t + \mathbf{b}_t, \quad (6)$$

where  $\mathbf{H}^{(q)} \in \mathbb{C}^{M_T \times \bar{N}}$  and  $\mathbf{G}^{(q)} \in \mathbb{C}^{M_R \times \bar{N}}$  correspond to the  $q$ -th block of  $\mathbf{H} \in \mathbb{C}^{M_T \times NQ}$  and  $\mathbf{G} \in \mathbb{C}^{M_R \times NQ}$ , respectively, defined as follows

$$\mathbf{H}^{(q)} = \mathbf{H}_{.[(q-1)\bar{N}+1, \dots, q\bar{N}]} \in \mathbb{C}^{M_T \times \bar{N}}, \quad q = 1, \dots, Q \quad (7)$$

$$\mathbf{G}^{(q)} = \mathbf{G}_{.[(q-1)\bar{N}+1, \dots, q\bar{N}]} \in \mathbb{C}^{M_R \times \bar{N}}, \quad q = 1, \dots, Q \quad (8)$$

Hence, the channel matrices can be seen as a concatenation of smaller submatrices such that  $\mathbf{H} = [\mathbf{H}^{(1)}, \dots, \mathbf{H}^{(Q)}] \in \mathbb{C}^{M_T \times NQ}$  and  $\mathbf{G} = [\mathbf{G}^{(1)}, \dots, \mathbf{G}^{(Q)}] \in \mathbb{C}^{M_R \times NQ}$ . Using the property (2), the noise-free received signal can be written as

$$\mathbf{y}_t = \sum_{q=1}^Q (\mathbf{x}_t^T \otimes \mathbf{I}_{M_R}) \text{vec}(\mathbf{G}^{(q)} \mathbf{S}_t^{(q)} \mathbf{H}^{(q)T}) \quad (9)$$

$$= \sum_{q=1}^Q (\mathbf{x}_t^T \otimes \mathbf{I}_{M_R}) (\mathbf{H}^{(q)} \otimes \mathbf{G}^{(q)}) \text{vec}(\mathbf{S}_t^{(q)}) \quad (10)$$

$$= \sum_{q=1}^Q (\text{vec}(\mathbf{S}_t^{(q)})^T \otimes \mathbf{x}_t^T \otimes \mathbf{I}_{M_R}) \mathbf{c}^{(q)}, \quad (11)$$

where  $\mathbf{c}^{(q)} = \text{vec}(\mathbf{H}^{(q)} \otimes \mathbf{G}^{(q)}) \in \mathbb{C}^{M_R M_T \bar{N}^2 \times 1}$ . By collecting the  $T$  time slots and removing the sum, we obtain

$$\mathbf{y} = [\mathbf{y}_1^T, \dots, \mathbf{y}_T^T]^T = [(\bar{\mathbf{S}} \diamond \mathbf{X})^T \otimes \mathbf{I}_{M_R}] \mathbf{c} \quad (12)$$

$$= [\boldsymbol{\Omega} \otimes \mathbf{I}_{M_R}] \mathbf{c} \in \mathbb{C}^{M_R M_T \times 1}, \quad (13)$$

where  $\boldsymbol{\Omega} = (\bar{\mathbf{S}} \diamond \mathbf{X})^T \in \mathbb{C}^{T \times M_T \bar{N}^2 Q}$  is the combined BD-RIS pilot matrix, which is known at the receiver, with  $\bar{\mathbf{S}} = [\mathbf{s}_1, \dots, \mathbf{s}_T] \in \mathbb{C}^{\bar{N}^2 Q \times T}$ ,  $\mathbf{s}_t = [\text{vec}(\mathbf{S}_t^{(1)})^T, \dots, \text{vec}(\mathbf{S}_t^{(Q)})^T]^T \in \mathbb{C}^{\bar{N}^2 Q \times 1}$ ,  $\mathbf{X} = [\mathbf{x}_1, \dots, \mathbf{x}_T] \in \mathbb{C}^{M_T \times T}$  is the pilot matrix, and  $\mathbf{c} = [\mathbf{c}^{(1)T}, \dots, \mathbf{c}^{(Q)T}]^T \in \mathbb{C}^{M_R M_T \bar{N}^2 Q \times 1}$  is the combined channel, for  $q = 1, \dots, Q$ . The classical approach is to estimate the combined channel  $\mathbf{c} \in \mathbb{C}^{M_R M_T \bar{N}^2 Q \times 1}$  resorts to a least squares (LS) method [18]. This problem can be formulated as

$$\hat{\mathbf{c}} = \underset{\mathbf{c}}{\text{argmin}} \|\mathbf{y} - (\boldsymbol{\Omega} \otimes \mathbf{I}_{M_R}) \mathbf{c}\|^2, \quad (14)$$

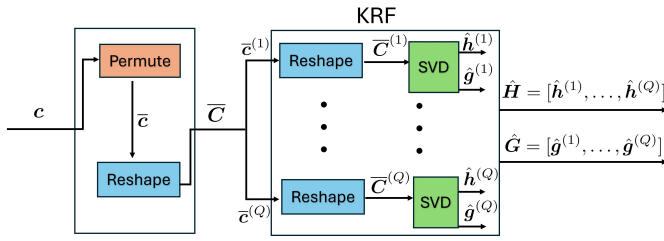


Fig. 2: Block diagram of the proposed KRF method.

from which the matching filter gives its solution as

$$\hat{\mathbf{c}} = \frac{\bar{N}}{T} (\mathbf{\Omega} \otimes \mathbf{I}_{M_R})^H \mathbf{y} \quad (15)$$

$$\approx \left[ \text{vec}(\mathbf{H}^{(1)} \otimes \mathbf{G}^{(1)})^T, \dots, \text{vec}(\mathbf{H}^{(Q)} \otimes \mathbf{G}^{(Q)})^T \right]^T$$

This solution requires  $T \geq M_T \bar{N}^2 Q$  to ensure a unique combined channel estimate. Next, we present the proposed solution for decoupling the estimates of  $\mathbf{G}$  and  $\mathbf{H}$  from the combined channel estimation  $\hat{\mathbf{c}}$ .

#### IV. DECOUPLED CHANNEL ESTIMATION METHOD

In this section, based on the LS estimate in (15), we show how to obtain the individual channel estimates.

Let us define the estimated combined channel matrix  $\hat{\mathbf{C}}$  as

$$\hat{\mathbf{C}} = \text{unvec}(\hat{\mathbf{c}})_{M_R M_T \bar{N}^2 \times Q} \quad (16)$$

$$\approx \left[ \text{vec}(\mathbf{H}^{(1)} \otimes \mathbf{G}^{(1)}), \dots, \text{vec}(\mathbf{H}^{(Q)} \otimes \mathbf{G}^{(Q)}) \right]. \quad (17)$$

The  $q$ -th column of  $\hat{\mathbf{C}}$  is given by  $\hat{\mathbf{c}}^{(q)} \approx \text{vec}(\mathbf{H}^{(q)} \otimes \mathbf{G}^{(q)}) \in \mathbb{C}^{M_R M_T \bar{N}^2 \times 1}$ . By applying property (4), we can define the permuted vector  $\bar{\mathbf{c}}^{(q)} = \mathbf{P} \hat{\mathbf{c}}^{(q)} \in \mathbb{C}^{M_R \bar{N} M_T \bar{N} \times 1}$  as

$$\bar{\mathbf{c}}^{(q)} \approx \text{vec}(\mathbf{H}^{(q)}) \otimes \text{vec}(\mathbf{G}^{(q)}), \quad (18)$$

where  $\mathbf{P} \in \mathbb{R}^{M_R \bar{N} M_T \bar{N} \times M_R M_T \bar{N}^2}$  is a permutation matrix. By collecting the  $Q$  group vectors, we have

$$\begin{aligned} \bar{\mathbf{C}} &= [\bar{\mathbf{c}}^{(1)}, \dots, \bar{\mathbf{c}}^{(Q)}] \in \mathbb{C}^{M_R \bar{N} M_T \bar{N} \times Q}, \\ &\approx [\mathbf{h}^{(1)} \otimes \mathbf{g}^{(1)}, \dots, \mathbf{h}^{(Q)} \otimes \mathbf{g}^{(Q)}] \\ &\approx \bar{\mathbf{H}} \diamond \bar{\mathbf{G}}, \end{aligned} \quad (19)$$

where  $\bar{\mathbf{H}} = [\mathbf{h}^{(1)}, \dots, \mathbf{h}^{(Q)}] \in \mathbb{C}^{M_T \bar{N} \times Q}$  and  $\bar{\mathbf{G}} = [\mathbf{g}^{(1)}, \dots, \mathbf{g}^{(Q)}] \in \mathbb{C}^{M_R \bar{N} \times Q}$ , with  $\mathbf{h}^{(q)} = \text{vec}(\mathbf{H}^{(q)})$  and  $\mathbf{g}^{(q)} = \text{vec}(\mathbf{G}^{(q)})$  being the vectorized forms of the  $q$ -th group of the channels  $\mathbf{G}$  and  $\mathbf{H}$ , respectively,  $\forall q = 1, \dots, Q$ . From the definition of the Khatri-Rao product in (1) and making use of (5), the  $q$ -th column of  $\bar{\mathbf{C}}$ , denoted as  $\bar{\mathbf{c}}^{(q)}$ , is reshaped into a rank-one matrix, i.e.,

$$\bar{\mathbf{C}}^{(q)} = \text{unvec}(\bar{\mathbf{c}}^{(q)})_{M_R \bar{N} \times M_T \bar{N}} \approx \mathbf{g}^{(q)} \mathbf{h}^{(q)T}, \quad (20)$$

To extract the individual channel estimates from (20), any rank-one matrix approximation method can be used, e.g., truncated singular value decomposition (SVD) or a power method. By assuming the rank-one approximation  $\bar{\mathbf{C}}^{(q)} \approx \sigma \mathbf{u}^{(q)} \mathbf{v}^{(q)H}$ , where  $\mathbf{u}^{(q)}$  and  $\mathbf{v}^{(q)}$  are the dominant left and right singular

#### Algorithm 1 Decoupled Channel Estimation based on Least-Squares Khatri-Rao Factorization (LS-KRF)

- 1: **Inputs:** Received signal  $\mathbf{y}$ , BD-RIS pilot matrix  $\mathbf{\Omega}$
- 2: Compute the LS estimate via a match filtering

$$\hat{\mathbf{c}} \approx \frac{\bar{N}}{T} (\mathbf{\Omega} \otimes \mathbf{I}_{M_R})^H \mathbf{y} \in \mathbb{C}^{M_R M_T \bar{N}^2 Q \times 1}$$

- 3: Permute the filtered signal:  $\bar{\mathbf{c}} = \mathbf{P} \hat{\mathbf{c}} \in \mathbb{C}^{M_R \bar{N} M_T \bar{N} Q \times 1}$ .
- 4: Obtain  $\bar{\mathbf{C}} = \text{unvec}(\bar{\mathbf{c}})_{M_R \bar{N} M_T \bar{N} \times Q} \approx [\mathcal{H}]_{(3)}^T \diamond [\mathcal{G}]_{(3)}^T$ .
- 5: **for**  $q = 1 : Q$  **do**
- 6: Let  $\bar{\mathbf{c}}^{(q)} \approx \mathbf{h}^{(q)} \otimes \mathbf{g}^{(q)} \in \mathbb{C}^{M_R \bar{N} M_T \bar{N} \times 1}$  be the  $q$ -th column of  $\bar{\mathbf{C}}$ . Obtain  $\bar{\mathbf{C}}^{(q)}$  as

$$\bar{\mathbf{C}}^{(q)} = \text{unvec}(\bar{\mathbf{c}}^{(q)})_{M_R \bar{N} \times M_T \bar{N}} \approx \mathbf{g}^{(q)} \mathbf{h}^{(q)T}$$

- 7: From the rank-one approximation (truncated SVD)  $\bar{\mathbf{C}}^{(q)} \approx \sigma^{(q)} \mathbf{u}^{(q)} \mathbf{v}^{(q)H}$ , obtain the channel estimates as

$$\hat{\mathbf{g}}^{(q)} = \sqrt{\sigma} \mathbf{u}^{(q)}, \quad \hat{\mathbf{h}}^{(q)} = \sqrt{\sigma} \mathbf{v}^{(q)*}$$

- 8: Define the  $q$ -th group channel matrices as

$$\hat{\mathbf{G}}^{(q)} = \text{unvec}(\hat{\mathbf{g}}^{(q)})_{M_R \times \bar{N}}, \quad \hat{\mathbf{H}}^{(q)} = \text{unvec}(\hat{\mathbf{h}}^{(q)})_{M_T \times \bar{N}}.$$

- 9: **end for**

- 10: **return**  $\hat{\mathbf{G}} = [\hat{\mathbf{G}}^{(1)}, \dots, \hat{\mathbf{G}}^{(Q)}]$  and  $\hat{\mathbf{H}} = [\hat{\mathbf{H}}^{(1)}, \dots, \hat{\mathbf{H}}^{(Q)}]$

vectors associated with the largest singular value  $\sigma$ , we obtain the channel estimates as

$$\hat{\mathbf{g}}^{(q)} = \sqrt{\sigma} \mathbf{u}^{(q)}, \quad \hat{\mathbf{h}}^{(q)} = \sqrt{\sigma} \mathbf{v}^{(q)*} \quad (21)$$

The estimates of the channel matrices are given by  $\hat{\mathbf{H}}^{(q)} = \text{unvec}(\hat{\mathbf{h}}^{(q)})_{M_T \times \bar{N}}$  and  $\hat{\mathbf{G}}^{(q)} = \text{unvec}(\hat{\mathbf{g}}^{(q)})_{M_R \times \bar{N}}$ . Repeating the process for the  $Q$  columns of  $\bar{\mathbf{C}}$  (corresponding to the  $Q$  BD-RIS groups), we build the complete channel matrices as  $\hat{\mathbf{H}} = [\hat{\mathbf{H}}^{(1)}, \dots, \hat{\mathbf{H}}^{(Q)}] \in \mathbb{C}^{M_T \times \bar{N} Q}$  and  $\hat{\mathbf{G}} = [\hat{\mathbf{G}}^{(1)}, \dots, \hat{\mathbf{G}}^{(Q)}] \in \mathbb{C}^{M_R \times \bar{N} Q}$ .

#### V. COMPUTATIONAL COMPLEXITY

The proposed KRF decoupled channel estimation method is an additional step to the LS combined channel estimator. By considering the matching filtering in (15), we have a computational cost of  $\mathcal{O}(M_R T^2)$ , where  $T = T_{\min} = M_T \bar{N}^2 Q$  is assumed. The KRF method requires computing  $Q$  rank-one approximations of an  $M_R \bar{N} \times M_T \bar{N}$  matrix. Assuming that for a matrix  $\mathbf{A}$  of size  $m \times n$ , the total complexity for its rank-one approximation is given by  $\mathcal{O}(mn)$  [20], the KRF method complexity is given by  $\mathcal{O}(M_R T)$ . Consequently, the computational complexity of the KRF method is given by  $\mathcal{O}(M_R T^2 + M_R T)$ . Note that the overall gap, in terms of computational complexity, between the LS and the KRF

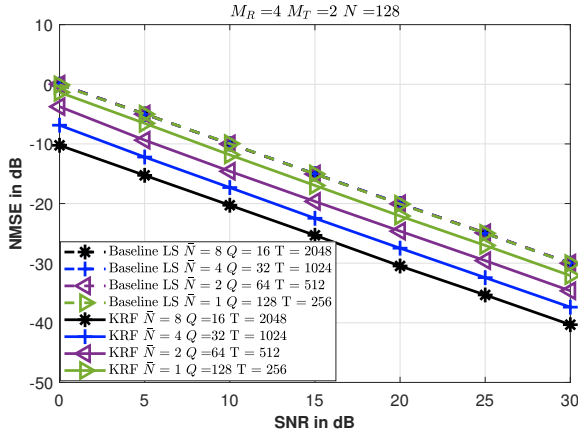


Fig. 3: NMSE performance varying the total pilot overhead  $T$ .

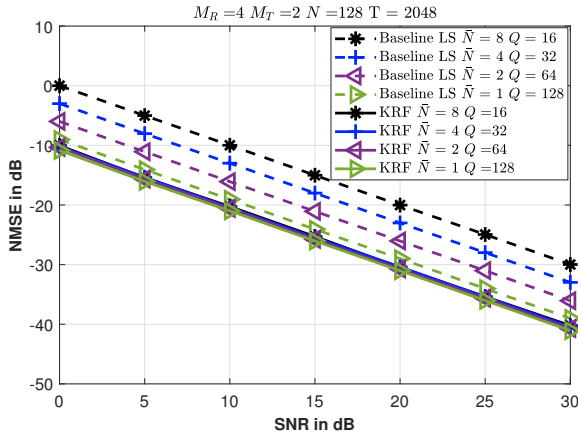


Fig. 4: NMSE performance by SNR fixing the pilot overhead  $T$ .

method becomes negligible since the bulk of the complexity is associated with the LS filtering stage. Also, notice that the  $Q$  rank-one approximation steps used in KRF (see Figure 2) can be executed in parallel, minimizing the processing delay associated with the decoupled channel estimation step.

## VI. SIMULATION RESULTS

In this section, we evaluate the performance of the proposed KRF method, comparing it with the baseline LS-based method [18] in terms of NMSE of the combined channel  $\mathbf{C} \in \mathbb{C}^{M_R M_T \times \tilde{N}^2 Q}$ , given by

$$\text{NMSE} = \frac{1}{L} \sum_{l=1}^L \frac{\|\mathbf{C}_{(l)} - \hat{\mathbf{C}}_{(l)}\|_F^2}{\|\mathbf{C}_{(l)}\|_F^2}$$

with  $L = 100$  being the number of trials. For the pilot sequence, we assume an orthogonal design by using a truncated discrete Fourier transform (DFT) structure for  $\mathbf{X} \in \mathbb{C}^{M_T \times T}$ , such that  $\mathbf{X}^H \mathbf{X} = T \mathbf{I}_{M_T}$ . Also, we adopt the orthogonal design of [18] for the BD-RIS training matrix  $\mathbf{S}$ .

Since the pilot overhead is given by  $T = M_T \tilde{N}^2 Q = M_T \tilde{N} N$ , the group size has the major impact. Thus, depending on the group size  $\tilde{N}$ , the pilot overhead changes even for

a fixed number of RIS elements  $N$ . In Figures 3 and 4, a RIS panel with  $N = 128$  elements is assumed. Starting with Figure 3, we evaluate the NMSE performance for different group sizes by setting the pilot sequence length to its minimum feasible value for each configuration, i.e.,  $T_{\min} = M_T \tilde{N}^2 Q$ . Note that the performance of the baseline LS method is insensitive to an increase in the group size (and thus pilot overhead) since it is based on the estimation of the combined channel only, whose number of channel coefficients ( $\tilde{N}^2 Q$ ) remains unchanged regardless of the group size. However, when including the KRF step to decouple the channel matrices, we observe that the performance increases with the group size  $\tilde{N}$ . This comes from the fact that the proposed method exploits the Kronecker structure of the combined channel in (14) after the LS filtering to decouple the channel matrices. This procedure yields refined channel estimates due to noise rejection obtained from the rank-one factorizations that are inherent to the KRF algorithm. In the end, this results in an improved accuracy of the reconstructed combined channel  $\hat{\mathbf{C}}$ .

In Figure 4, we fix the training overhead to  $T = 2048$  (the minimum value for the configuration with  $\tilde{N} = 8$ ). We can observe that the baseline LS method offers an improved performance as the group size  $\tilde{N}$  is reduced. Indeed, for a fixed training overhead  $T$ , when the group size  $\tilde{N}$  becomes smaller, the total number of channel coefficients is decreased accordingly. Therefore, we can conclude that the single-connected architecture ( $\tilde{N} = 1$ ) is preferable for channel estimation when the LS method is used. On the other hand, the proposed KRF method exhibits approximately the same performance for all the considered group sizes. This is due to the fact that our channel decoupling method refines the combined channel estimate at the output of the LS stage by extracting the individual estimates of the involved channels through multiple rank-one factorizations. This procedure benefits from a noise rejection gain that increases when the group size  $\tilde{N}$  becomes larger [8]. In addition, as shown in Fig. 4, smaller group sizes  $\tilde{N}$  are compensated by larger training lengths  $T$ , yielding approximately the same performance for all configurations.

In Fig. 5, we observe that the LS keeps approximately a constant gain by varying the numbers  $M_R$  and  $M_T$  of receive and transmit antennas, while the KRF performance is enhanced when  $M_R$  and/or  $M_T$  increases, being able to extract more accurate channel estimates as higher levels of transmit/receive spatial diversities are available. This remarkable result corroborates the effectiveness of the decoupled BD-RIS channel estimation, which benefits from noise rejection gains provided by the rank-one approximation steps of the KRF algorithm.

In Fig. 6, the performances are compared for a fixed SNR of 20 dB and a fixed training overhead  $T = 1024$ . Here, we point out that by varying the number of BD-RIS elements  $N = \tilde{N} Q$ , the performance gap of the proposed method between single-connected architecture ( $\tilde{N} = 1$ ) and the group-connected architecture ( $\tilde{N} > 1$ ) is negligible when the proposed method is used. In contrast, the NMSE performance of the LS receiver significantly depends on the connection degree of the BD-RIS, exhibiting performance gaps between the single-connected and

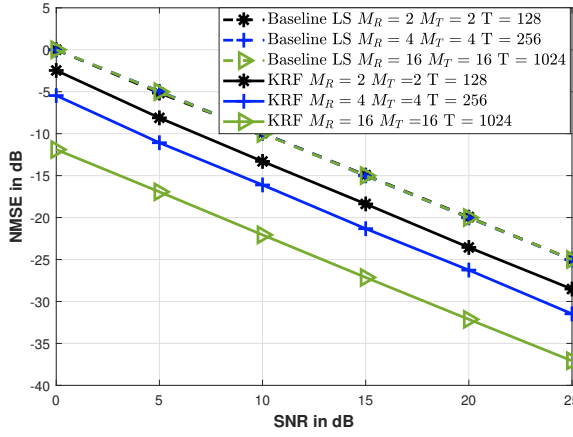


Fig. 5: NMSE performance for  $N = 32$ ,  $\bar{N} = 2$ , and  $Q = 16$ .

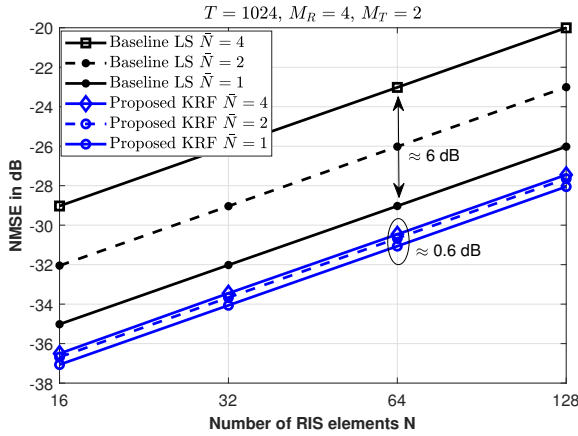


Fig. 6: NMSE varying the number of RIS elements.

the group-connected architectures.

## VII. CONCLUSIONS

We have proposed a decoupled channel estimation method for BD-RIS assisted systems. Our method efficiently exploits the intrinsic Kronecker structure of the combined channel by performing simple permute and reshape operations to filtered signals, allowing the extraction of individual channel estimates via multiple independent rank-one approximations. As shown in our numerical results, decoupling the combined channel estimate into its constituent individual components provides remarkable gains over the baseline LS estimation scheme while offering similar performances regardless of the connection degree of the BD-RIS for fixed training overheads.

## REFERENCES

- [1] E. Basar, M. Di Renzo, J. De Rosny, M. Debbah, M.-S. Alouini, and R. Zhang, "Wireless communications through reconfigurable intelligent surfaces," *IEEE Access*, vol. 7, pp. 116 753–116 773, Aug. 2019.
- [2] M. Jian, G. C. Alexandropoulos, E. Basar, C. Huang, R. Liu, Y. Liu, and C. Yuen, "Reconfigurable intelligent surfaces for wireless communications: Overview of hardware designs, channel models, and estimation techniques," *Intelligent Conv. Networks*, vol. 3, 2022.

- [3] S. Shen, B. Clerckx, and R. Murch, "Modeling and architecture design of Reconfigurable Intelligent Surfaces using scattering parameter network analysis," *IEEE Transactions on Wireless Communications*, vol. 21, no. 2, pp. 1229–1243, 2022.
- [4] H. Li, S. Shen, M. Nerini, and B. Clerckx, "Reconfigurable intelligent surfaces 2.0: Beyond diagonal phase shift matrices," *IEEE Communications Magazine*, vol. 62, no. 3, pp. 102–108, 2024.
- [5] H. Li, S. Shen, and B. Clerckx, "Beyond diagonal reconfigurable intelligent surfaces: From transmitting and reflecting modes to single-, group-, and fully-connected architectures," *IEEE Transactions on Wireless Communications*, vol. 22, no. 4, pp. 2311–2324, 2023.
- [6] A. L. Swindlehurst, G. Zhou, R. Liu, C. Pan, and M. Li, "Channel estimation with reconfigurable intelligent surfaces—A general framework," *Proc. of the IEEE*, vol. 110, no. 9, pp. 1312–1338, 2022.
- [7] B. Zheng, C. You, W. Mei, and R. Zhang, "A survey on channel estimation and practical passive beamforming design for intelligent reflecting surface aided wireless communications," *IEEE Comm. Surv. & Tutorials*, vol. 24, no. 2, pp. 1035–1071, 2022.
- [8] G. T. de Araújo, A. L. F. de Almeida, and R. Boyer, "Channel estimation for intelligent reflecting surface assisted MIMO systems: A tensor modeling approach," *IEEE J. Sel. Topics Signal Process.*, vol. 15, no. 3, pp. 789–802, Feb. 2021.
- [9] G. T. de Araújo and A. L. F. de Almeida, "Parafac-based channel estimation for intelligent reflective surface assisted mimo system," in *2020 IEEE 11th Sensor Array and Multichannel Signal Processing Workshop (SAM)*, 2020, pp. 1–5.
- [10] A. L. F. de Almeida, G. Favier, and J. C. M. Mota, "PARAFAC-based unified tensor modeling for wireless communication systems with application to blind multiuser equalization," *Signal Processing*, vol. 87, no. 2, pp. 337–351, 2007.
- [11] —, "A constrained factor decomposition with application to MIMO antenna systems," *IEEE Transactions on Signal Processing*, vol. 56, no. 6, pp. 2429–2442, 2008.
- [12] G. Favier and A. L. F. de Almeida, "Overview of constrained PARAFAC models," *EURASIP Journal of Advances in Signal Processing*, vol. 2014, no. 142, pp. 1–25, Sep. 2014.
- [13] —, "Tensor space-time-frequency coding with semi-blind receivers for MIMO wireless communication systems," *IEEE Transactions on Signal Processing*, vol. 62, no. 22, pp. 5987–6002, 2014.
- [14] L. Wei, C. Huang, G. C. Alexandropoulos, C. Yuen, Z. Zhang, and M. Debbah, "Channel estimation for RIS-empowered multi-user MISO wireless communications," *IEEE Trans. Commun.*, vol. 69, no. 6, pp. 4144–4157, 6 2021.
- [15] K. Ardah, S. Ghorekhloo, A. L. F. de Almeida, and M. Haardt, "TRICE: A channel estimation framework for RIS-aided millimeter-wave MIMO systems," *IEEE Signal Processing Letters*, vol. 28, pp. 513–517, 2021.
- [16] K. B. A. Benício, A. L. F. de Almeida, B. Sokal, Fazal-E-Asim, B. Makki, and G. Fodor, "Tensor-based channel estimation and data-aided tracking in IRS-assisted MIMO systems," *IEEE Wireless Communications Letters*, vol. 13, no. 2, pp. 333–337, 2024.
- [17] B. Sokal, P. R. B. Gomes, A. L. F. de Almeida, B. Makki, and G. Fodor, "Reducing the control overhead of intelligent reconfigurable surfaces via a tensor-based low-rank factorization approach," *IEEE Transactions on Wireless Communications*, vol. 22, no. 10, pp. 6578–6593, 2023.
- [18] H. Li, S. Shen, Y. Zhang, and B. Clerckx, "Channel estimation and beamforming for beyond diagonal reconfigurable intelligent surfaces," *IEEE Transactions on Signal Processing*, vol. 72, pp. 3318–3332, 2024.
- [19] A. L. F. de Almeida, B. Sokal, H. Li, and B. Clerckx, "Channel estimation for beyond diagonal RIS via tensor decomposition," *arXiv preprint arXiv:2407.20402*, 2024.
- [20] N. Kishore Kumar and J. Schneider, "Literature survey on low rank approximation of matrices," *Linear and Multilinear Algebra*, vol. 65, no. 11, pp. 2212–2244, 2017.